Journal of Molecular Structure 1018 (2012) 21–27

Contents lists available at SciVerse ScienceDirect

Journal of Molecular Structure

journal homepage: www.elsevier.com/locate/molstruc

Structure of 2,3-dicarboxy-1-methylpyridinium chloride studied by X-ray diffraction, DFT calculation, NMR, FTIR and Raman spectra

P. Barczyński, M. Szafran *, M. Ratajczak-Sitarz, Ł. Nowaczyk, Z. Dega-Szafran, A. Katrusiak

Faculty of Chemistry, Adam Mickiewicz University, Grunwaldzka 6, 60780 Poznań, Poland

ARTICLE INFO

Article history:
Available online 29 November 2011

Keywords:
2,3-Dicarboxy-1-methylpyridinium chloride
X-ray diffraction
B3LYP calculations
FTIR and NMR spectra
Hydrogen bonds
Electrostatic interactions

ABSTRACT

The structure of 2,3-dicarboxy-1-methylpyridinium chloride (**1**) has been studied by X-ray diffraction, DFT calculations, NMR, FTIR and Raman spectra. The crystals are monoclinic, space group $P2_1/c$. Chloride anion links two 2,3-dicarboxy-1-methylpyridinium cations into infinite zigzag chains down the [0 0 1] direction by the OH···Cl⁻···HO hydrogen bonds of 2.970(2) and 3.011(2) Å. Hydrogen bond lengths in single molecules (**2**–**4**) optimized by the B3LYP/6-311++G(d,p) approach depend on the environment and intramolecular O·H·O hydrogen bond. Linear correlations between the experimental ^{13}C and ^{1}H chemical shifts (δ_{exp}) of the investigated compound in DMSO-d_6 and the GIAO/B3LYP/6-311++G(d.p) magnetic isotropic shielding constants (σ_{calc}) calculated using the screening solvation model (COSMO), $\delta_{exp} = a + b\ \sigma_{calc,}$ are reported. The FTIR spectrum of the solid compound is consistent with the X-ray structure. The deformation in-plane and out-of-plane OH vibrations, both in FTIR and second-derivative (d^2) spectra, appear as two bands consistent with the OH···Cl⁻···HO arrangement.

1. Introduction

The crystal structure of 2,3-pyridinedicarboxylic acid (quinolinic acid) was determined by X-ray [1] and neutron diffractions [2,3]. Quinolinic acid in the crystal is zwitterion (betaine) with one acidic hydrogen atom transferred to the nitrogen atom. The second acidic hydrogen atom is involved in a short intramolecular and asymmetric OHO hydrogen bond of 2.398(3) Å.

Pyridine carboxylic acids, at first heated with methyl iodide [4–6] or methyl sulfate [7] and then subjected to treatment with propylene oxide [8,9] or ion-exchange resins, Dovex-22C [5,9] or Amberlite [4], convert to carboxy-1-methylpyridinum inner salts (betaines).

In our earlier works, we have described H-bonding and electrostatic interactions in the structures of homarinium chloride [10], trigonellinium chloride [11], 4-carboxy-1-methylpyridinium chloride [12] and 3,4-dicarboxy-1-methylpyridinium chloride [13]. In this work we have synthesized 2,3-dicarboxy-1-methylpyridinium chloride (Scheme 1) and characterized it by single-crystal X-ray diffraction, FTIR, Raman and NMR spectroscopy and by DFT calculations.

2. Experimental and calculations

2.1. 2,3-Diethoxycarbonylpyridine

2,3-Pyridinedicarboxylic acid (10 g) and thionyl chloride (20 cm^3) were refluxed for 2 h. Excess of thionyl chloride was evaporated. To the yellow crystals obtained, absolute ethanol (20 cm^3) was added and the contents were refluxed for 1 h. Then ethanol was distilled off, the residue was treated with a water solution of potassium carbonate to pH 7.7–8.0, extracted with diethyl ether (5×30 cm^3), and dried with magnesium sulfate. The solvent was distilled off and the residue redistilled under vacuum, (153 °C/1.2 mm Hg, 167–170/6 mm Hg [14] and yield 87%).

2.2. 2,3-Diethoxycarbonyl-1-methylpyridinium iodide

To 2,3-diethoxycarbonylpyridine (9.7 g) methyl iodide (15 g) was added and left for 4 days at room temperature. The excess of methyl iodide was evaporated and the solid yellow residue recrystallized from a 1:1 mixture of n-hexane with n-butanol; m.p. 134 °C, yield 87%. Elemental analysis calculated for $C_{12}H_{16}INO_4$: %N 3.84, %C 39.47, %H 4.42; found: %N 3.79, %C 39.38, %H 4.58.

2.3. 2,3-Diethoxycarbonyl-1-methylpyridinium nitrate

2,3-Diethoxycarbonyl-1-methylpyridinium iodide (5 g) was converted into its nitrate salt by adding aqueous solution of silver nitrate (2.3 g). Silver iodide was filtered off, water from filtrate evaporated under reduced pressure and to the solid residue absolute ethanol was added. Solvent was evaporated and the residue was recrystallized from isopropanol, m.p. 130–131 °C, yield 79%. Elemental analysis calculated for $C_{12}H_{16}N_2O_7$: %N 9.33, %C 48.00, %H 5.37; found: %N 9.27, %C 47.83, %H 5.57.

* Corresponding author. Tel.: +48 61 8291320; fax: +48 61 8291505.
E-mail address: szafran@amu.edu.pl (M. Szafran).

0022-2860/$ - see front matter © 2011 Published by Elsevier B.V.
doi:10.1016/j.molstruc.2011.11.009

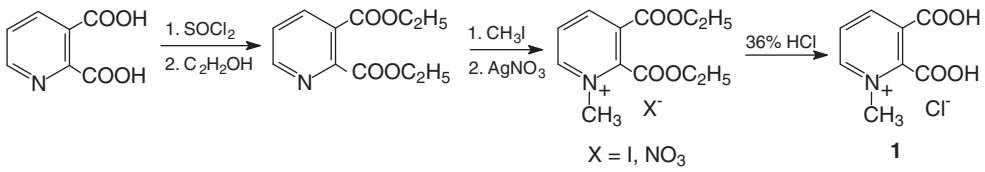

Scheme 1. Synthesis of 2,3-dicarboxy-1-methylpyridinium chloride (**1**) from 2,3-pyridinedicarboxylic acid.

2.4. 2,3-Dicarboxy-1-methylpyridinium chloride (*1*)

A portion of 5 g of 2,3-diethoxycarbonyl-1-methylpyridinium nitrate was heated under reflux with excess of 36% aqueous hydrochloride for 12 h. After cooling 3.2 g of 2,3-dicarboxy-1-methylpyridinium chloride was separated and the crude white crystals were recrystallized from methanol, m.p. 236–238 °C. Elemental analysis: calculated for $C_8H_8ClNO_4$: %N 6.44, %C 44.16, %H 3.71; found: %N 6.35, %C 43.90, %H 3.84.

2.5. Measurements and calculations

The crystals (**1**) were stable under normal conditions and the X-ray diffraction measurements were carried out on an Oxford Diffraction Super Nova diffractometer using Cu Kα radiation at room temperature: ω-scan data collection with $\Delta\omega = 1^\circ$ frames and 40 s exposures were applied. The structure was solved by direct methods using SHELXS-97 program and refined on F^2 by full-matrix least-squares with the SHELXL-97 program [15]. Two acidic H-atoms at O(1) and O(3) were located from difference Fourier maps and refined with isotropic temperature factors. The positions of all other hydrogen atoms were determined from molecular geometry (C—H distances of 0.93 and 0.96 Å) and their U_{iso}'s were related to the thermal vibrations of their carriers. The crystal data, together with the details concerning data collection and structure refinement are given in Table 1 and the atomic coordinates in Table 2. The parameters in the CIF form are available as Electronic Supplementary Information from the Cambridge Crystallographic Database Centre (842381). Molecular illustrations were prepared using programs ORTEPII [16] and XP [17].

FTIR spectra were recorded in Nujol and Fluorolube suspension between KBr plates on a Bruker IFS 66v/S spectrometer, evacuated to avoid water and CO_2 absorptions, at a 2 cm^{-1} resolution. Each FTIR spectrum was measured by acquisition of 64 scans. The Raman spectrum of crystalline sample was measured on a Bruker

Table 1
Crystal data and structure refinement for 2,3-dicarboxy-1-methylpyridinium chloride (**1**).

Empirical formula	$C_8H_8ClNO_4$
Formula weight	217.60
Temperature	293(2)
Wavelength	1.54178 Å
Crystal system	Monoclinic
Space group	$P2_1/c$
Unit cell dimensions	a = 7.3767(2) Å
	b = 11.2790(2) Å
	c = 11.4339(2) Å
	β = 101.590(2)°
Volume	931.92(3) Å^3
Z	4
Calculated density	1.551 g cm^{-3}
Absorption coefficient	3.585 mm^{-1}
$F(000)$	448
Crystal size	0.25 × 0.20 × 0.15 mm
θ range for data collection	5.57–73.96°
Max/min. indices h,k,l	$-8 \leqslant h \leqslant 5$, $-14 \leqslant k \leqslant 13$, $-14 \leqslant l \leqslant 13$
Reflections collected/unique	6436/1846 R_{int} = 0.0115
Completeness to θ_{max} = 73.96°	98.1%
Refinement method	Full-matrix least-squares on F^2
Data/restraints/parameters	1846/0/135
Goodness-of-fit on F^2	1.048
Final R indices [$I > 2\sigma_I$]	R_1 = 0.0443, wR_2 = 0.1305
R indices (all data)	R_1 = 0.0446, wR_2 = 0.1307
Largest diff. peak and hole	0.560 and −0.294 eÅ^{-3}

Table 2
Atomic coordinates (×10^4) and equivalent isotropic displacement parameters (Å^2 × 10^3) for 2,3-dicarboxy-1-methylpyridinium chloride (**1**). $U_{(eq)}$ is defined as one third of the trace of the orthogonalized U_{ij} tensor.

Atom	x	y	z	U_{eq}/U_{iso}
Cl(1)	3204(1)	−5232(1)	1434(1)	50(1)
N(1)	1975(2)	−4647(2)	7732(2)	37(1)
C(2)	2126(3)	−4329(2)	6616(2)	33(1)
C(3)	2498(3)	−5189(2)	5828(2)	34(1)
C(4)	2712(3)	−6360(2)	6202(2)	41(1)
C(5)	2531(3)	−6655(2)	7347(2)	47(1)
C(6)	2164(3)	−5782(2)	8096(2)	45(1)
C(7)	1673(4)	−3740(2)	8614(2)	53(1)
C(8)	1817(3)	−3024(2)	6309(2)	37(1)
C(9)	2622(3)	−4827(2)	4584(2)	37(1)
O(1)	3367(2)	−2434(2)	6540(2)	51(1)
O(2)	294(2)	−2639(2)	5966(2)	53(1)
O(3)	3284(3)	−5667(2)	4006(2)	54(1)
O(4)	2138(4)	−3880(2)	4186(2)	77(1)
H(71)	1596	−4121	9353	80
H(72)	542	−3321	8313	80
H(73)	2688	−3191	8747	80
H(4)	2976	−6943	5685	50
H(5)	2657	−7439	7605	56
H(6)	2044	−5976	8868	54
H(1)	3180(50)	−1760(40)	6500(30)	88(13)
H(3)	3180(50)	−5460(30	3250(40)	97(13)

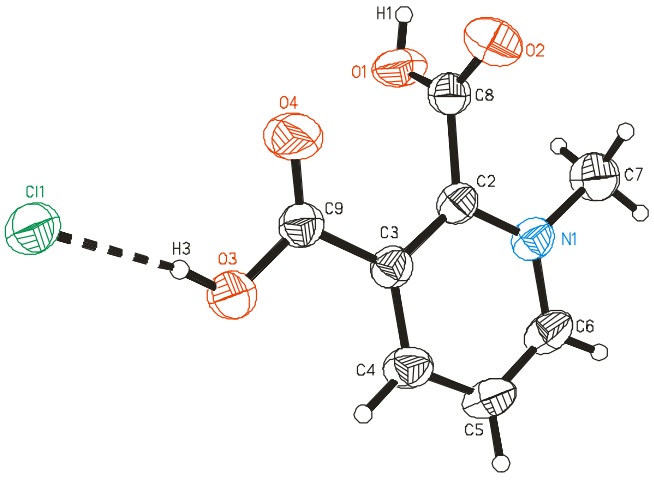

Fig. 1. Atom numbering for 2,3-dicarboxy-1-methylpyridinium chloride (**1**). The hydrogen bond is indicated by the dashed line, and the thermal ellipsoids are drawn at the 50% probability level.

Table 3
X-ray and calculated bond lengths (Å), bond and torsion angles (°) for 2,3-dicarboxy-1-methylpyridinium chloride.

Parameter	X-ray	B3LYP/6-311++G(d,p)		
	1	**2**	**3** DMSO	**4** DMSO
Bond lengths				
N(1)—C(2)	1.352(3)	1.3601	1.3568	1.3622
N(1)—C(6)	1.345(3)	1.3563	1.3515	1.3517
N(1)—C(7)	1.484(3)	1.4837	1.4883	1.4899
C(2)—C(3)	1.388(3)	1.3879	1.3907	1.4022
C(2)—C(8)	1.520(3)	1.5217	1.5220	1.5438
C(3)—C(4)	1.388(3)	1.3912	1.3974	1.3982
C(3)—C(9)	1.500(3)	1.5410	1.5065	1.5154
C(4)—C(5)	1.384(3)	1.3939	1.3873	1.3852
C(5)—C(6)	1.367(3)	1.3782	1.3793	1.3769
O(1)—C(8)	1.303(3)	1.3431	1.3280	1.2670
O(2)—C(8)	1.195(3)	1.2027	1.2034	1.2304
O(3)—C(9)	1.305(3)	1.2495	1.3166	1.3038
O(4)—C(9)	1.187(3)	1.2406	1.2147	1.2287
Bond angles				
N(1)—C(2)—C(3)	119.5(2)	120.339	120.138	118.770
N(1)—C(6)—C(5)	120.9(2)	121.012	121.072	121.266
N(1)—C(2)—C(8)	116.0(2)	117.431	116.508	117.219
C(7)—N(1)—C(2)	120.7(2)	120.203	120.331	121.025
C(7)—N(1)—C(6)	117.8(2)	119.118	118.688	117.188
C(2)—N(1)—C(6)	121.4(2)	120.674	120.979	121.781
C(2)—C(3)—C(4)	119.4(2)	119.184	118.983	119.204
C(2)—C(3)—C(9)	118.9(2)	118.332	119.417	125.516
C(3)—C(4)—C(5)	119.6(2)	119.771	119.852	120.383
C(3)—C(2)—C(8)	124.5(2)	122.129	123.289	123.946
C(4)—C(3)—C(9)	121.8(2)	122.476	121.599	115.279
C(4)—C(5)—C(6)	119.2(2)	119.014	118.975	118.517
O(1)—C(8)—O(2)	127.6(2)	125.958	126.539	128.683
O(1)—C(8)—C(2)	111.3(2)	111.133	111.385	114.672
O(2)—C(8)—C(2)	121.0(2)	121.516	121.898	116.640
O(3)—C(9)—O(4)	125.0(2)	132.194	125.873	121.207
O(3)—C(9)—C(3)	112.5(2)	114.164	112.357	120.332
O(4)—C(9)—C(3)	122.5(2)	113.641	121.771	118.397
Torsion angles				
N(1)—C(2)—C(3)—C(4)	−0.2(3)	−0.59	0.04	3.09
N(1)—C(2)—C(3)—C(8)	178.7(2)	178.42	179.90	−176.52
N(1)—C(2)—C(8)—O(1)	91.4(2)	94.38	91.90	126.82
N(1)—C(2)—C(8)—O(2)	−84.8(2)	−72.90	−83.56	−53.89
N(1)—C(6)—C(5)—C(4)	0.2(3)	−0.13	0.04	1.64
C(7)—N(1)—C(2)—C(3)	176.9(2)	−179.32	−179.69	177.77
C(7)—N(1)—C(2)—C(8)	−4.7(3)	−2.92	−2.51	−5.05
C(7)—N(1)—C(6)—C(5)	−176.9(2)	179.70	179.63	179.79
C(2)—N(1)—C(6)—C(5)	0.5(3)	0.53	0.06	−1.09
C(6)—N(1)—C(2)—C(3)	−0.4(3)	−0.17	−0.12	−1.32
C(6)—N(1)—C(2)—C(8)	178.0(2)	176.23	177.06	175.86
C(2)—C(3)—C(4)—C(5)	0.8(3)	0.98	0.10	−2.53
C(3)—C(4)—C(5)—C(6)	−0.8(3)	−0.63	−0.16	0.20
C(4)—C(3)—C(2)—C(8)	−178.5(2)	−176.82	−176.94	−173.89
C(5)—C(4)—C(3)—C(9)	−178.1(2)	−177.98	−179.76	177.10
C(8)—C(2)—C(3)—C(9)	0.4(3)	2.19	2.92	6.51
O(1)—C(8)—C(2)—C(3)	−19.2(2)	−89.29	−91.02	−56.16
O(2)—C(8)—C(2)—C(3)	93.5(3)	103.43	93.52	123.13
O(3)—C(9)—C(3)—C(2)	168.9(2)	176.05	179.79	26.31
O(3)—C(9)—C(3)—C(4)	−12.2(3)	−4.98	−1.36	−153.31
O(4)—C(9)—C(3)—C(2)	−12.0(3)	−4.34	−1.32	−156.59
O(4)—C(9)—C(3)—C(4)	166.9(2)	174.63	178.54	23.80

FRA-106/S instrument operating at the 1064 nm exciting line of Nd:YAG laser, with the resolution of 1 cm^{-1}. The spectrum was measured by acquisition of 200 scans.

NMR spectra in DMSO-d_6 solution relative to TMS were recorded on a Bruker Advance DRX spectrometer operating at 599.93 and 150.85 MHz for ^1H and ^{13}C, respectively.

The DFT calculations were performed using the Gaussian 03 program package [18]. The calculations employed the B3LYP exchange–correlation functional, which combines the hybrid functional of Becke [19,20] with the gradient-correlation functional of Lee et al. [21] and the split-valence polarized 6-311++G(d,p) basis set [22]. The X-ray geometry of **1** was used as a starting point of the calculations. The magnetic isotropic shielding constants were calculated using the standard GIAO/B3LYP/6-311++G(d,p) (Gauge-Independent Atomic Orbital) approach with the Gaussian 03 program package using the conductor-like screening solvation model (COSMO) [23–25].

3. Results and discussion

3.1. Crystal structure

The molecular structure and atom numbering of 2,3-dicarboxy-1-methylpyridinium chloride (**1**) are shown in Fig. 1. The bond lengths, bond and torsion angles determined in the X-ray study are summarized in Tables 3 and 4.

The linking of cations and anions is governed by hydrogen bonds OH···Cl^-···HO, forming infinite zigzag chains down the [001] direction, as illustrated in Fig. 2, and by electrostatic attractions. The ribbon-like chains are arranged in such a manner that the chloride anions are located close to the nitrogen atoms in pyridine rings of the neighboring ribbons located below and above in the [100] direction. The Cl^-···N distances are 3.495(2) and 4.121(2) Å, while four short Cl^-···HC contacts (Cl^-···H distance from 2.74 to 3.29 Å) are formed to the pyridine and methyl H-atoms of two cations along the (100) plane. Thus each Cl^- anion is sixfold coordinated by cations, two of which are OH···Cl bonded and four others attracted electrostatically (Table 4). An analogous octahedral coordination arrangement of six Cl^- anions is formed about each of the cations (Fig. 3). The angles between pyridine ring and carboxylate groups at 2 and 3 positions are 87.5(1)° and 12.3(2)°, respectively; the angle between the two carboxyl groups is 84.9(3)°.

3.2. Optimized structures

The structures of the molecules optimized by the B3LYP/6-311++G(d,p) approach of monomers in vacuum (**2**) and DMSO (**3** and **4**) are shown in Fig. 4. The calculated geometrical parameters, total energies and dipole moments of the optimized molecules are listed in Tables 3 and 4. In **2** (vacuum) and **4** (DMSO) the hydrogen bonded proton is linked with chloride atom (Cl—H···O(3)), while in **3** (DMSO) the structure is similar to that in the crystal (Cl···H—O(3)). In **4** the intramolecular O(3)—H···O(1) hydrogen bond is present. The energy of **3** is by 9.57 kcal/mol lower in comparison to that in **4**. In **3** the angles between pyridine ring and carboxylate groups at 2 and 3 positions are 82.3° and 1.3°, respectively, while the angle between the two carboxyl groups is 106.8°.

3.3. ^{13}C and ^1H NMR spectra

The ^{13}C and ^1H chemical shifts for **1** in DMSO-d_6 are listed in Table 5. The relations between the experimental ^{13}C and ^1H chemical shifts (δ_{exp}) and Gauge Inducting Atomic Orbitals (GIAO) isotropic magnetic shielding constants (σ_{calc}, Table 5) calculated for the optimized structures **3** and **4**, which are now widely used [26–28], are usually linear and described by the following equation: $\delta_{exp} = a + b\ \sigma_{calc}$. The slope and intercept of the least-square correlation lines are used to scale the GIAO isotropic magnetic shielding constants, σ, and to predict the chemical shifts, $\delta_{pred} = a + b\ \sigma_{calc}$ (Fig. 5). As shown by the data in Table 5, the agreement between the experimental and calculated data is satisfactory both for carbon-13 and hydrogen. The r.m.s. data for **4** are lower than for **3**, which suggests

Table 4
Energies (Hartree, a.u.), dipole moments (μ, Debye), hydrogen bond distances (Å), the shortest intermolecular contacts (Å), angels (°) in the crystals (**1**), vacuum (**2**) and DMSO (**3**–**4**) for 2,3-dicarboxy-1-methylpyridinium chloride.

Compounds	Energy	μ	D–H···A	D–H	H···A	D···A	D–H···A	$N^+\cdots Cl^-$
X-ray								
1			O(3)—H(3)···Cl(1)	0.88(5)	2.10(5)	2.970(2)	171	7.4663[b]
			O(1)—H(1)···Cl(1)[a]	0.77(4)	2.25(4)	3.011(2)	169	3.495(2)[c]
								4.121(2)[c]
								4.199(2)[d]
B3LYP/6-311++G(d,p)								
2 Vacuum	−1125.7351966	17.5222	Cl(1)—H···O(3)	1.3444	1.6418	2.9805	172.92	7.6290[b]
3 DMSO	−1125.8076926	32.4765	O(3)—H(3)···Cl(1)	1.0120	1.9823	2.9831	169.57	7.5542[b]
4 DMSO	−1125.7924472	19.2640	Cl(1)—H···O(4)	1.3424	1.6499	2.9888	174.50	7.6194[b]
			O(3)—H···O(1)	1.0300	1.4774	2.4856	164.64	

Symmetry codes:
[a] $x, -0.5-y, -0.5+z$.
[b] x, y, z.
[c] $-x, -y-1, -z+1$.
[d] $x, y, z+1$.

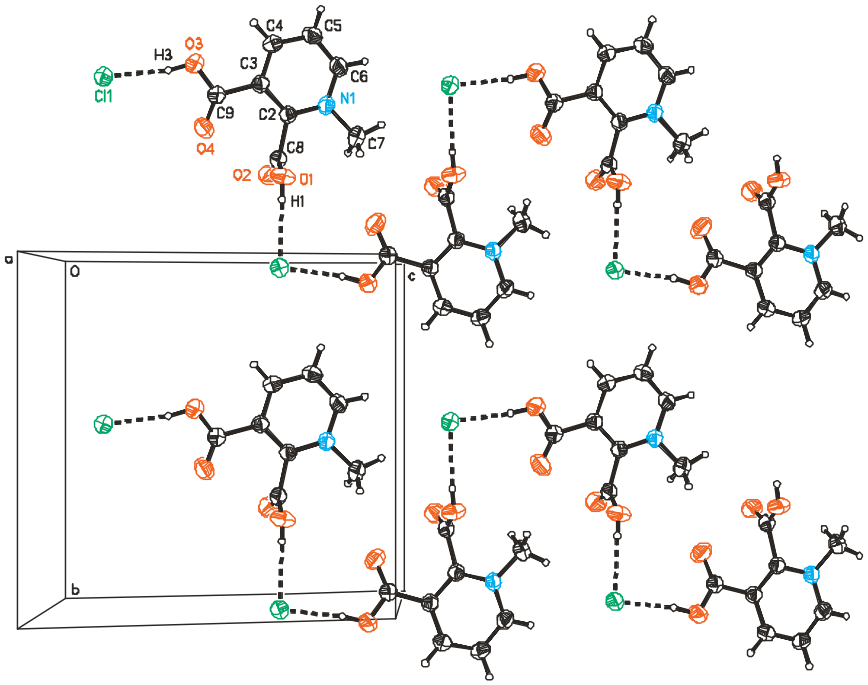

Fig. 2. Autostereographic projection [35] of two chains of hydrogen bonded ionic pairs in the crystal structure of (**1**). The hydrogen bonds are indicated by the dashed line, and the thermal ellipsoids are shown at the 50% probability level.

that in DMSO solution the intramolecular O·H·O hydrogen bond is formed.

3.4. FTIR and Raman spectra

The FTIR spectra of **1** and its deuterated analog measured in the solid state are shown in Fig. 6a and frequencies are listed in Table 6. The broad and strong absorption with three maxima at 2709, 2562 and 2467 cm^{-1} arise from the νOH stretching vibration. In the Raman spectrum, the intensity of this absorption is much weaker (Fig. 6c). In the spectrum of deuterated sample the νOD bands are located at 2087, 1990 and 1926 cm^{-1}. In general the FTIR spectra of the compounds investigated are similar to those of 3,4-dicarboxy-1-methylpyridinium chloride and its deuterated sample [13].

The fine structure of the νOH and νOD absorptions observed in the investigated chlorides are generated by the strong anharmonic coupling mechanism, in which the most prominent role is played by the high frequency proton stretching vibration νAH, anharmonically coupled with the low frequency A—H···B hydrogen bond stretching vibration ν(A—H···B) [29,30]. Further contribution to the absorption is brought by the Fermi resonance between the overtones and νAH vibration [31].

The intense doublets at 1750 and 1729 cm^{-1} correspond to the νC=O vibrations. In deuterated complex these bands are shifted to 1747 and 1725 cm^{-1}. In Raman spectrum the single νC=O band is at 1725 cm^{-1}.

In the spectrum of **1** the OH deformation in-plane and out-of-plane vibrations appear as doublets at 1398 and 1381 cm^{-1} (βOH) and 890 and 868 cm^{-1} (γOH) which on deuteration are shifted to 1028, 1016 and 635, 626 cm^{-1}, respectively. The absorption at

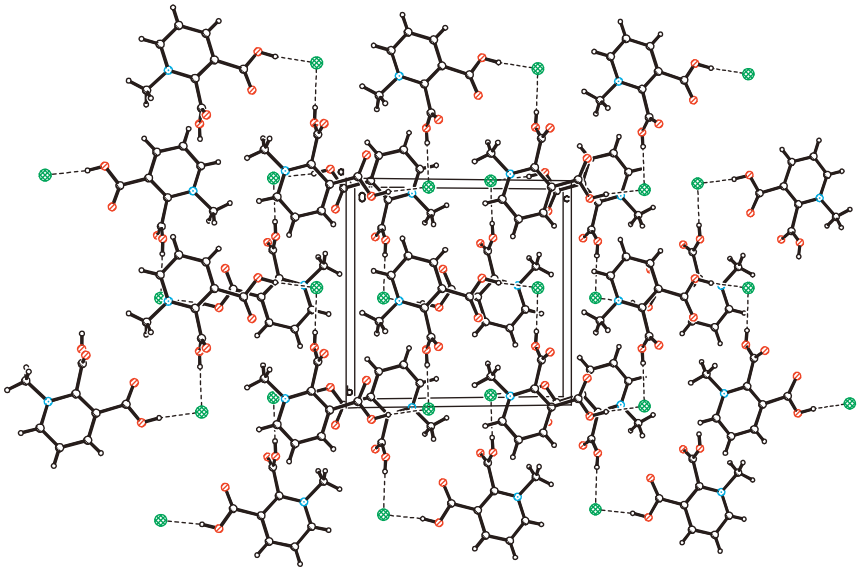

Fig. 3. Autostereographic projection [35] of the ionic packing in crystal structure of 2,3-dicarboxy-1-methylpyridinium chloride. The hydrogen bonds are indicated by the dashed line.

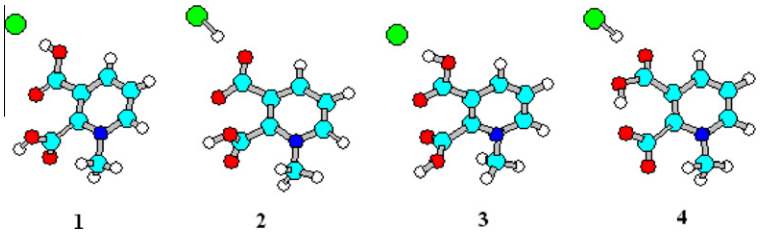

Fig. 4. Comparison of the X-ray (**1**) and B3LYP/6-311++G(d,p) (**2**–**4**) structures of 2,3-dicarboxy-1-methylpyridinium chloride.

Table 5
Experimental, predicted ($\delta_{pred} = a + b\ \sigma_{calc}$) carbon-13 and proton chemical shifts (ppm) and calculated GIAO/B3LYP/6-311G(d,p) isotropic magnetic shielding constants (σ_{calc}) for 2,3-dicarboxy-1-methypyridinium chloride in DMSO.

Atom[a]	δ_{exp}	δ_{pred} (**3**)	δ_{pred} (**4**)	σ_{calc} (**3**)	σ_{calc} (**4**)
Carbon					
C(2)	149.47	148.15	151.28	27.6592	23.1598
C(3)	128.29	129.70	127.11	46.9872	48.3205
C(4)	146.67	148.31	147.58	27.4888	27.0114
C(5)	127.26	128.82	124.28	47.9166	51.2630
C(6)	149.25	147.62	147.16	28.2136	27.4530
C(7)	46.54	45.87	47.93	134.8489	130.7285
C(8)OO	161.21	161.62	161.36	13.3969	12.6663
C(9)OO	163.02	161.49	165.02	13.6755	6.8635
a[b]				174.5361	173.5333
b[c]				−0.9541	−0.9608
r[d]				0.9993	0.9988
Av. dif.[e]		0.02	−0.02		
R.m.s[f]		1.44	1.91		
Proton					
H(4)	8.98 (d)	8.96	9.42	22.4128	22.7277
H(5)	8.24 (dd)	9.03	8.23	22.3254	23.8791
H(6)	9.28 (d)	8.39	8.78	23.0737	23.3457
NCH_3	4.33	4.46	4.39	27.8359	27.9142
				27.4893	26.9951
				27.5507	27.9214
NCH_3 av				27.6253	27.6102
a[b]				28.3030	32.8075
b[c]				−0.8632	−1.0291
r[d]				0.9532	0.9858
Av. dif.[e]		−0.003	−0.003		
R.m.s[f]		0.69	0.39		

[a] Numbering of atoms is given in Fig. 1.
[b] Intercept.
[c] Slope.
[d] Correlation coefficient.
[e] Average (signed) differences between experimental and predicted chemical shifts.
[f] Root-mean-square errors.

higher frequencies corresponds to the shorter OH···Cl^- hydrogen bonds. Two bands of deformation OH and OD vibrations are in good agreement with the X-ray data.

In the second-derivative spectra, d^2, the minima have the same wavenumbers as the maxima in the absorbance spectra [29,32–34]. The intensity of relative amplitudes of bands in d^2 spectra varies inversely to the square of their half-width ratio. The half-widths of the νOH and νOD bands are too large and therefore intensities of these bands in the d^2 spectra are very weak (Fig. 6b).

The band at 1227 cm^{-1} in the spectrum of **1** which disappears on deuteration (Fig. 6a) does not correspond to a fundamental transition, but it should be assigned to a combination of skeletal vibrations with γOH. An analogous new band at 1335 cm^{-1} in the deuterated IR spectrum should be a combination of skeletal vibrations with βOD.

4. Conclusions

The molecular and crystal structures of 2,3-dicarboxy-1-methylpyridinium chloride (**1**) have been determined by X-ray diffraction and the B3LYP/6-311++G(d,p) calculations. In the crystal, each Cl^- ion is engaged in two hydrogen bonds with the COOH groups of two molecules, OH···Cl^-···HO, of 2.970(2) and 3.011(2) Å. According to the B3LYP/6-311++G(d,p) calculations, in molecule **2** (vacuum) and **4** (DMSO) the hydrogen bonded proton is linked with chlorine atom, Cl—H···O, while in **3** (DMSO) the Cl^- anion interacts with COOH group, similarly as in the crystal (Cl^-···H—O). The correlations between the experimental ^{13}C and ^1H chemical shifts in DMSO-d_6 and the isotropic magnetic shielding constants obtained by the GIAO/B3LYP/6311++G(d,p)

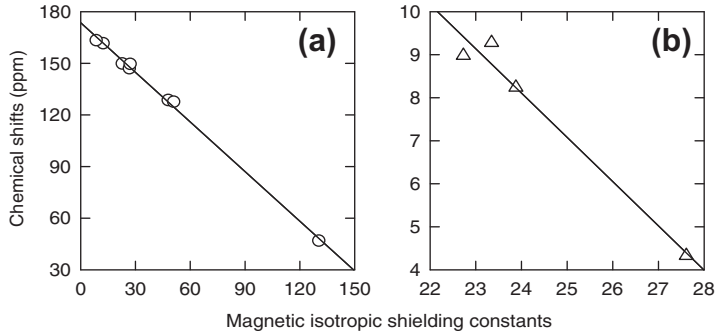

Fig. 5. Plot of the experimental chemical shifts in DMSO-d_6 (δ_{exp}) vs. the magnetic isotropic shielding constants (σ_{calc}) from the GIAO/B3LYP/6-311++G(d,p) calculations for 2,3-dicarboxy-1-methylpyridinium chloride (**3**) in DMSO; (a) carbon-13, (b) proton.

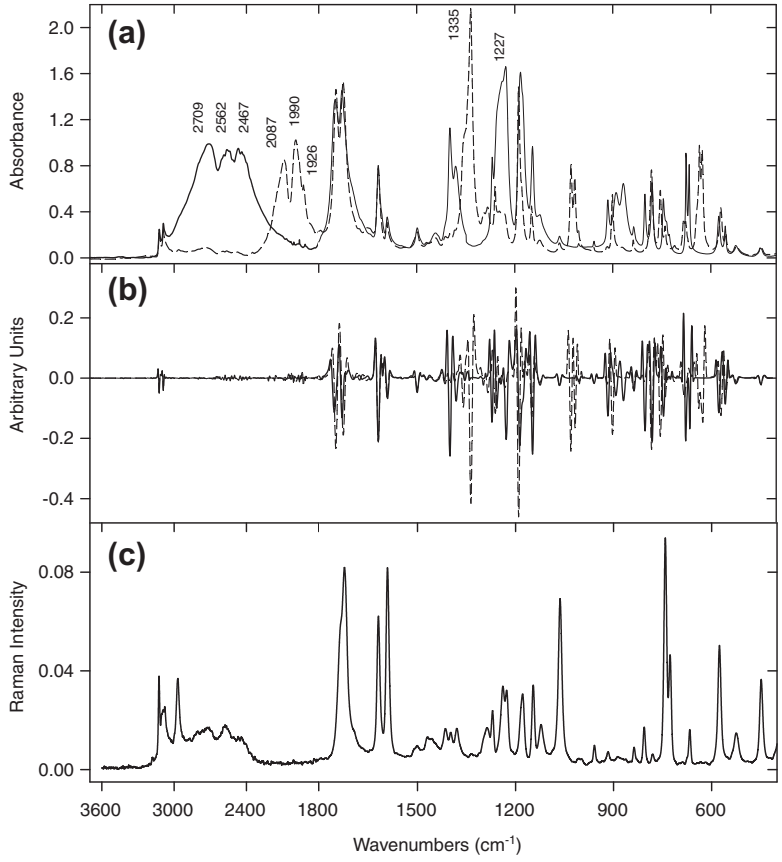

Fig. 6. Spectra of 2,3-dicarboxy-1-methylpyridinium chloride (**1**): (a) FTIR spectra in Nujol and Fluorolube, (b) second-derivative spectra, and (c) Raman spectrum in solid state. Dashed line denotes spectra of deuterated sample.

Table 6
Experimental vibrational data for 2,3-dicarboxy-1-methylpyridinium chloride.

Raman	FTIR		Aproximate assign.[a]
H	H	D	
3181			νCH
3127	3123	3124	νCH
3104			νCH
3093	3089	3089	νCH_3
3079			νCH_3
2971			νCH_3
2800–2400	2900–2300	2100–1900	νOH/νOD
1725	1750	1747	νC=O
	1729	1725	νC=O
1621	1618	1617	νCC
1594	1590	1591	νCC

Table 6 (*continued*)

Raman	FTIR		Aproximate assign.[a]
1503	1498	1498	βCH
1471			νCC
1458	1442	1442	νCC
1416			νCC
1400	1398	1028	βOH/βOD
1381	1381	1016	βOH/βOD
1289		1282	βCH
1272	1267	1260	νCN
1241	1238	1233	βCH
1229	1227	1335	νCC + γOH/γOD
1180	1182	1188	βCH_3, βCH
1148	1146	1148	βCH_3
1124	1123	1124	νCC
1066			βCH_3
960	957		γCH
919	915	901	νCN, νCC
	890	635	γOH/γOD
	868	626	γOH/γOD
839	839	837	Ring, νCN
808	802	802	Ring, νCN
	780	781	Ring, νCN
744	745	754	τCO
729	727	740	γCH
669	675	689	Ring + βCO
	666	677	Ring + βCO
578	576	569	Ring + βCO
	556	554	Ring + βCO
527	524	521	Ring + βCO
450	448	447	Ring + νCN

[a] Abbreviations: ν, stretching; β, deformation in plane; γ, deformation out-of-plane; τ, torsion.

approaches are linear with good correlation coefficients. The broad bands in the 2900–2400 cm^{-1} region correspond to the OH stretching vibrations. In the Raman spectrum, the intensity of this absorption is much weaker. The half-width of this absorption is too large and in the d^2 spectrum the corresponding negative peak is very weak. The deformation in-plane and out-of-plane OH modes, both in FTIR and d^2 spectra, appear as two bands corresponding to two $OH\cdots Cl^-$ bonds. In FTIR spectrum there are two bands corresponding to the νC═O vibration, while only one in Raman spectrum.

Acknowledgment

The calculations were performed at the Poznań Supercomputing and Networking Centre.

References

[1] F. Takusagawa, K. Hirotsu, A. Shimada, Bull. Chem. Soc. Jpn. 46 (1973) 2372.
[2] A. Kvick, T.F. Koetzle, R. Thomas, F. Takusagawa, J. Chem. Phys. 60 (1974) 3866.
[3] F. Takusagawa, T.F. Koetzle, Acta Cryst. B34 (1978) 1149.
[4] E.F. Smissman, G. Hite, J. Am. Chem. Soc. 81 (1959) 1201.
[5] E.M. Kosower, J.W. Patton, J. Org. Chem. 26 (1961) 1318.
[6] M. Szafran, A. Katrusiak, Z. Dega-Szafran, J. Mol. Struct. 934 (2009) 79.
[7] X.B. Wang, J.E. Dactres, X. Yang, K.M. Broadus, L. Lis, L.S. Wang, S.R. Kass, J. Am. Chem. Soc. 125 (2003) 296.
[8] R.E. Phillips, R.L. Soulten, J. Chem. Educ. 72 (1995) 624.
[9] P. Barczyński, A. Katrusiak, J. Koput, M. Szafran, J. Mol. Struct. 889 (2008) 394.
[10] M. Szafran, J. Koput, Z. Dega-Szafran, A. Katrusiak, J. Mol. Struct. 700 (2004) 109.
[11] M. Szafran, J. Koput, Z. Dega-Szafran, A. Katrusiak, M. Pankowski, K. Stobiecka, Chem. Phys. 289 (2003) 201.
[12] M. Szafran, J. Koput, Z. Dega-Szafran, A. Katrusiak, J. Mol. Struct. 797 (2006) 66.
[13] M. Szafran, A. Katrusiak, Z. Dega-Szafran, P. Barczyński, J. Mol. Struct. 934 (2009) 79.
[14] V.I. Trubnikov, L.M. Malakhova, E.S. Zhadanovich, N.A. Preabrazhenskii, Pharm. Chem. J. 1 (1967) 680.
[15] G.M. Sheldrick, Acta Crystallogr. A64 (2008) 112.
[16] C.K. Johnson, ORTEPII. Report ORNL-5138, Oak Ridge National Laboratory, Tennessee, USA, 1976.
[17] Stereochemical Workstation Operation Manual, Release 3.4, Siemens Analytical X-ray Instruments INC. Madison, 1989.
[18] M.J. Frisch, G.W. Trucks, H.B. Schlegel, G.E. Scuseria, M.A. Robb, J.R. Cheeseman, J.A. Montgomery, Jr., T. Vreven, K.N. Kudin, J.C. Burant, J.M. Millam, S.S. Iyengar, J. Tomasi, V. Barone, B. Mennucci, M. Cossi, G. Scalmani, N. Rega, G.A. Petersson, H. Nakatsuji, M. Hada, M. Ehara, K. Toyota, R. Fukuda, J. Hasegawa, M. Ishida, T. Nakajima, Y. Honda, O. Kitao, H. Nakai, M. Klene, X. Li, J.E. Knox, H.P. Hratchian, J.B. Cross, C. Adamo, J. Jaramillo, R. Gomperts, R.E. Stratmann, O. Yazyev, A.J. Austin, R. Cammi, C. Pomelli, J.W. Ochterski, P.Y. Ayala, K. Morokuma, G.A. Voth, P. Salvador, J.J. Dannenberg, V.G. Zakrzewski, S. Dapprich, A.D. Daniels, M.C. Strain, O. Farkas, D.K. Malick, A.D. Rabuck, K. Raghavachari, J.B. Foresman, J.V. Ortiz, Q. Cui, A.G. Baboul, S. Clifford, J. Cioslowski, B.B. Stefanov, G. Liu, A. Liashenko, P. Piskorz, I. Komaromi, R.L. Martin, D.J. Fox, T. Keith, M.A. Al-Laham, C.Y. Peng, A. Nanayakkara, M. Challacombe, P.M.W. Gill, B. Johnson, W. Chen, M.W. Wong, C. Gonzalez, J.A. Pople, GAUSSIAN 03, Revision B.05, Gaussian, Inc., Pittsburgh PA, 2003.
[19] A.D. Becke, J. Chem. Phys. 98 (1993) 5648.
[20] A.D. Becke, J. Chem. Phys. 107 (1997) 8554.
[21] C. Lee, W. Yang, C.R. Parr, Phys. Rev. B 37 (1988) 785.
[22] W.J. Hehre, L. Random, P.v.R. Schleyer, J.A. Pople, Ab Initio Molecular Orbital Theory, Wiley, New York, 1989.
[23] V. Barone, M. Cossi, J. Phys. Chem. A 112 (1998) 1995.
[24] G. Brancato, N. Rega, W. Barone, J. Chem. Phys. 123 (2006) 164515.
[25] K. Wolinski, J.F. Hilton, P. Pulay, J. Am. Chem. Soc. 112 (1990) 8251 (and references cited therein).
[26] A. Forsych, A.B. Sabag, J. Am. Chem. Soc. 119 (1997) 9483.
[27] B. Ośmiałowski, E. Kolehmainen, R. Gawinecki, Magn. Res. Chem. 39 (2001) 334 (and references cited therein).
[28] A.R. Katritzky, N.G. Akhmedov, A. Güven, E.F.V. Scriven, S. Majumder, R.G. Akhmedova, C.D. Hall, J. Mol. Struct. 783 (2006) 191.
[29] S. Bratos, H. Ratajczak, P. Viot, in: J.C. Dore, J. Teixeire (Eds.), Hydrogen Bonded Liquids, Kluger Academic Publisher, 1991, p. 221 (and references cited therein).
[30] H. Ratajczak, W.J. Orville-Thomas (Eds.), Molecular Interactions, vol. 1, Wiley, New York, 1980.
[31] S. Bratos, D. Hadži, J. Chem. Phys. 27 (1957) 991.
[32] G. Talsky, Derivative Spectroscopy, VGR, Weinheim, 1994.
[33] W.I. Buder, D.W. Hopkins, Photochem. Photobiol. 12 (1970) 439.
[34] W.F. Maddams, M.J. Southon, Spectrochim. Acta 38A (1982) 459.
[35] A. Katrusiak, J. Mol. Graph. Model. 19 (2001) 363.